

LETTER • OPEN ACCESS

## Asymmetric impacts of El Niño and La Niña on the Pacific–North American teleconnection pattern: the role of subtropical jet stream

To cite this article: Ya Wang *et al* 2021 *Environ. Res. Lett.* **16** 114040

View the [article online](#) for updates and enhancements.

You may also like

- [Development of High Throughput X-ray detectors using Superconducting Tunnel Junctions with a large area size](#)  
Y Fujisawa, G Fujii, M Ukibe et al.

- [Improving the spatial resolution of superconducting tunnel junction THz wave detectors using a modified LiNbO<sub>3</sub> absorber](#)  
M Sone, N Igarashi, M Naruse et al.

- [Characteristics of Nb/AI superconducting tunnel junctions fabricated using ozone gas](#)  
Masahiro Ukibe, Go Fujii and Masataka Ohkubo

# ENVIRONMENTAL RESEARCH LETTERS



## OPEN ACCESS

RECEIVED  
16 May 2021

REVISED  
27 September 2021

ACCEPTED FOR PUBLICATION  
21 October 2021

PUBLISHED  
8 November 2021

Original content from  
this work may be used  
under the terms of the  
[Creative Commons  
Attribution 4.0 licence](#).

Any further distribution  
of this work must  
maintain attribution to  
the author(s) and the title  
of the work, journal  
citation and DOI.



## LETTER

# Asymmetric impacts of El Niño and La Niña on the Pacific–North American teleconnection pattern: the role of subtropical jet stream

Ya Wang<sup>1,4</sup> Kaiming Hu<sup>1,2,3,\*</sup> Gang Huang<sup>1,2,4,\*</sup> and Weichen Tao<sup>1</sup>

<sup>1</sup> State Key Laboratory of Numerical Modeling for Atmospheric Sciences and Geophysical Fluid Dynamics, Institute of Atmospheric Physics, Chinese Academy of Sciences, Beijing, People's Republic of China

<sup>2</sup> Laboratory for Regional Oceanography and Numerical Modeling, Qingdao National Laboratory for Marine Science and Technology, Qingdao, 266237, People's Republic of China

<sup>3</sup> Center for Monsoon System Research, Institute of Atmospheric Physics, Chinese Academy of Sciences, Beijing, People's Republic of China

<sup>4</sup> University of Chinese Academy of Sciences, Beijing, 100049, People's Republic of China

\* Authors to whom any correspondence should be addressed.

E-mail: [hkm@mail.iap.ac.cn](mailto:hkm@mail.iap.ac.cn) and [hg@mail.iap.ac.cn](mailto:hg@mail.iap.ac.cn)

**Keywords:** Pacific–North American (PNA) teleconnection pattern, El Niño/Southern Oscillation (ENSO), asymmetry, subtropical jet stream (STJ)

Supplementary material for this article is available [online](#)

## Abstract

The asymmetric impacts of El Niño and La Niña on the Pacific–North American teleconnection pattern in boreal winter have important implications for the surface air temperature and precipitation anomalies in North America. Previous studies have shown that the varying tropical convective heating contributes to the zonal shift of the teleconnection pattern during different El Niño/Southern Oscillation phases. In this study, using reanalysis, atmospheric general circulation model (AGCM) simulations, and a linear baroclinic model, we further present that the discrepancy of the subtropical jet stream (STJ) during El Niño and La Niña also contributes to the asymmetry. The atmospheric anomalies readily extract kinetic energy and effectively develop at the exit of the STJ. During El Niño (La Niña) years, as the central-eastern tropical Pacific warms up (cools down), the meridional temperature gradient in central subtropical Pacific increases (decreases), leading to the eastward (westward) shift of the STJ. The movement of the STJ leads to the shift of the location where disturbance develops most efficiently, ultimately contributing to the asymmetry of the teleconnection pattern.

## 1. Introduction

As the dominant interannual air-sea coupled mode in the tropical Pacific, the El Niño/Southern Oscillation (ENSO) has profound effects on global climate variability, and is the major seasonal predictability source, especially for North America (Horel and Wallace 1981, Hoerling *et al* 1997, Trenberth *et al* 1998, Liu and Alexander 2007, Tao *et al* 2016, Xie *et al* 2016, Adames and Wallace 2017, Hu *et al* 2019, Yang and Huang 2021). The predictability mainly takes roots in the tropical convection and the associated Pacific–North American (PNA) teleconnection pattern. The teleconnection pattern triggered by ENSO in boreal winter features a wave structure from the tropical Pacific to North America, modulating the strength of the Aleutian Low and high-pressure center in western

Canada, and causing extreme weather events over North America (Horel and Wallace 1981, Hoerling *et al* 1997, Trenberth *et al* 1998, Liu and Alexander 2007, Johnson and Kosaka 2016).

Many previous studies have found that the impacts of El Niño and La Niña on the PNA teleconnection pattern are not symmetric (Hoerling *et al* 1997, Mo *et al* 1998, Rao and Ren 2016, Trascasa-Castro *et al* 2019). Hoerling *et al* (1997) presented that the wave exhibits a westward shift during La Niña years relative to that during El Niño years, which further leads to significant differences in the regions influenced by ENSO in the United States. The zonal movement of anomalous tropical deep convection is considered to be responsible for the zonal shift. Besides, the atmospheric responses during El Niño years are found to be stronger than

that during La Niña. Utilizing idealized symmetric sea surface temperature (SST) anomalies with the same spatial distribution, Trascasa-Castro *et al* (2019) found that atmospheric anomalies forced by La Niña are four times weaker than that forced by El Niño of the equivalent magnitude. The nonlinear responses of convective activities to positive and negative SST anomalies play an important role in the inconsistent intensities of atmospheric responses (Gadgil *et al* 1984, Hoerling *et al* 1997, Rao and Ren 2016).

The aforementioned studies highlight the importance of tropical convective anomalies to the zonal movement of the teleconnection pattern. Are there other factors that also contribute to the zonal movement of the atmospheric circulations? The Rossby wave trains triggered by ENSO are influenced not only by tropical convective heating, but also by the basic mean flow (Simmons *et al* 1983, Hoskins *et al* 1985, Ting and Yu 1998, Held *et al* 2002, Kosaka and Nakamura 2006, Hu *et al* 2019). Simmons *et al* (1983) pioneered that the subtropical jet stream (STJ) plays an important role in the development of the Rossby wave trains in the subtropics. Ting and Yu (1998) further presented that the STJ could anchor the zonal location of the tropical heating-excited wave train. Besides, observed evidence shows that ENSO strongly affects the STJ. The STJ intensifies and shifts equatorial-ward during El Niño winters and vice versa in La Niña winters (Seager *et al* 2003, Hu *et al* 2021). Do the different responses of the STJ to La Niña and El Niño further affect the ENSO teleconnection?

In this study, we will investigate whether the asymmetric PNA-like teleconnection patterns excited by El Niño and La Niña are related to the STJ, and how the STJ modulates the wave train from the energy conversion perspective. The rest of this study is organized as follows, section 2 introduces data and models. Section 3 presents the observed asymmetric ENSO teleconnections. The mechanism that leads to the asymmetry will be presented in section 4. Section 5 provides a summary.

## 2. Data and models

In this study, monthly mean geopotential height and surface air temperature (SAT) are derived from the National Centers for the Environmental Prediction–Department of Energy (NCEP-DOE) atmospheric Reanalysis 2 (NCEP2; Kanamitsu *et al* 2002) at a resolution of  $2.5^\circ \times 2.5^\circ$  from 1979 to 2015. The global gridded monthly (SST) datasets from extended reconstructed sea surface temperature (ERSST.v5 SST) are utilized (Huang *et al* 2017). ENSO is measured by the December–January–February (DJF) mean Niño3.4 ( $5^\circ\text{S}$ – $5^\circ\text{N}$ ,  $170^\circ\text{W}$ – $120^\circ\text{W}$ ) SST index. An El Niño (A La Niña) event is defined when the DJF Niño3.4 index is greater (less) than 0.5 ( $-0.5$ )  $^\circ\text{C}$ . Strong ENSO events with Niño3.4 index greater (less) than 1 ( $-1$ )  $^\circ\text{C}$  are selected in this study,

as the atmospheric response to strong ENSO events is more pronounced than weak ENSO events (e.g. Jia *et al* 2016). The composite analysis is used in the study, and the statistical significance is evaluated by the two-tailed Student's *t*-test.

The Max Planck Institute for Meteorology atmospheric general circulation model (ECHAM5.3.2) is employed in this study, with a triangular truncation at zonal wave-number 63 (T63; equivalent to  $1.9^\circ$  horizontal resolution) and 31 vertical levels extending to 10 hPa. A more detailed description of this model can be found in Roeckner *et al* (2003).

The linear baroclinic model (LBM) used in this study is based upon the primitive equations linearized at a given state. We utilize a T42L20 dry version of LBM, with a horizontal resolution of T42 and 20 sigma levels, a horizontal and vertical diffusion, Rayleigh friction, and Newtonian damping. The horizontal diffusion has an e-folding damping time scales of 6 h for the smallest wave, and the Rayleigh friction and Newtonian damping have a scale of  $1\text{ day}^{-1}$  for  $\sigma < 0.9$ ,  $5\text{ day}^{-1}$  for  $\sigma < 0.89$ ,  $15\text{ day}^{-1}$  for sigma level of  $\sigma < 0.83$ ,  $30\text{ day}^{-1}$  for  $0.03 < \sigma < 0.83$ , and  $1\text{ day}^{-1}$  for  $\sigma > 0.89$ . More details of the model are presented in Watanabe and Kimoto (2000). To produce a stable atmospheric response to the heating forcing, the model is integrated for 50 d, and averages from 20 to 50 d are used.

## 3. Asymmetric responses of El Niño and La Niña

### 3.1. The asymmetry in reanalysis and model simulations

Figures 1(a) and (b) present the composite upper-level geopotential height anomalies in boreal winter during El Niño years (1982/1983, 1986/1987, 1991/1992, 1994/1995, 1997/1998, 2009/2010) and La Niña years (1984/1985, 1988/1989, 1998/1999, 1999/2000, 2007/2008, 2010/2011). Note that only strong ENSO events with Niño3.4 index greater (less) than 1 ( $-1$ )  $^\circ\text{C}$  are selected (see section 2). During El Niño (La Niña) years, as the tropical eastern Pacific warms up (cools down), the upper-level atmospheric circulation forms an equatorially symmetric high (low) anomaly in the tropics. Anomalies further develop in extratropics, with low (high) centers in the north Pacific, and high (low) centers in North America, featuring a wave fluctuation. The pattern correlation coefficient (PCC) among  $0^\circ\text{N}$ – $60^\circ\text{N}$  and  $180^\circ\text{W}$ – $40^\circ\text{W}$  of the composites with the PNA wave train (figure S1 (available online at [stacks.iop.org/ERL/16/114040/mmedia](https://stacks.iop.org/ERL/16/114040/mmedia)), defined as the second empirical orthogonal function (EOF) mode of 200 hPa geopotential height in the Northern Hemisphere) is 0.90 and  $-0.96$ , respectively. Area weight is considered in calculating PCC. In addition to the similarity of the spatial pattern revealed by the PCC, the wave active flux (WAF) shows similar

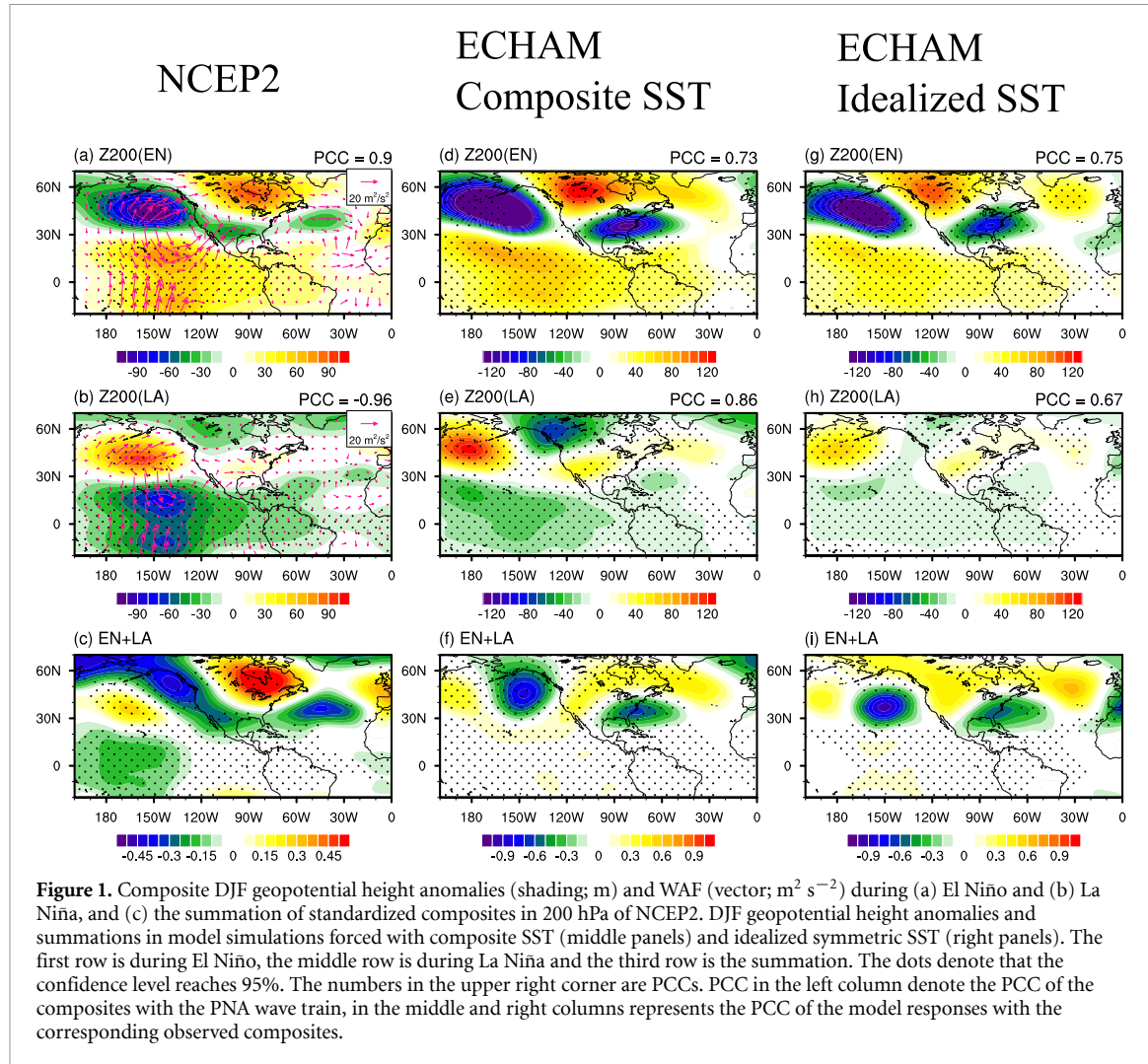


**Figure 1.** Composite DJF geopotential height anomalies (shading; m) and WAF (vector;  $m^2 s^{-2}$ ) during (a) El Niño and (b) La Niña, and (c) the summation of standardized composites in 200 hPa of NCEP2. DJF geopotential height anomalies and summations in model simulations forced with composite SST (middle panels) and idealized symmetric SST (right panels). The first row is during El Niño, the middle row is during La Niña and the third row is the summation. The dots denote that the confidence level reaches 95%. The numbers in the upper right corner are PCCs. PCC in the left column denote the PCC of the composites with the PNA wave train, in the middle and right columns represents the PCC of the model responses with the corresponding observed composites.

characteristics of wave propagation from the subtropical Pacific to North America during different ENSO phases.

The composites during El Niño and La Niña years share similar spatial pattern and wave propagation characteristics. However, the extratropical atmospheric responses to El Niño are more eastward relative to La Niña (figures 1(a) and (b)). In the subtropical North Pacific, the atmospheric anomaly is centered at 150 °W (160 °W) in El Niño (La Niña). The downstream positive atmospheric anomalies mainly distribute in the Mideast of Canada during El Niño (figure 1(a)), accompanied by the anomalous high SAT (figure S2(a)). The corresponding negative geopotential height anomalies over North America in La Niña shift about 30-longitude degrees westward relative to their counterparts in El Niño (figure 1(b)), and pronounced cooling is found over Alaska and western Canada (figure S2(b)). Figure 1(c) presents the summation of the two composites standardized by dividing the composite anomalies by the maximum or minimum value of the anomaly center over the North Pacific (between 30 °N–60 °N and 160 °W–120 °W). The summation shows significant negative geopotential height anomalies along the

west coast of North America and positive anomalies over the central North Pacific, further indicating the asymmetric responses of atmospheric circulation to El Niño and La Niña. Given the asymmetric modulation of ENSO teleconnection by the interdecadal Pacific oscillation (IPO; Dong *et al* 2018), we also composite geopotential height after the component linearly related to the IPO index (Henley *et al* 2015) is removed (figure S3). The movement of the ENSO teleconnection is still significant, indicating that the result is robust.

ECHAM5.3.2 simulations forced with composite SST anomalies (figure S4) have been conducted to further investigate the mechanism involved in the asymmetric circulation responses. Three sets of experiments with different boundary conditions have been conducted to investigate the issue. The control run (hereafter CTL) is forced by the climatological SST and sea ice for the period 1980–2005. The other two sensitive experiments are El Niño run and La Niña run. We first composite the DJF seasonal mean SST anomalies in El Niño years, and then add them to climatological SST for every calendar month to force the El Niño run, so does that in the La Niña run. Each experiment is integrated for 21 years,

the final 20 years were utilized for analysis. Thus, each simulation is equivalent to 20 member ensemble runs. Ensemble-mean results for DJF calculated as the deviations from CTL are analyzed. The observed asymmetric atmospheric responses to El Niño and La Niña are well reproduced by model simulations (figures 1(d)–(f)).

Note that the composite El Niño SST anomalies are stronger and somewhat more eastward relative to that during La Niña (figure S4). As many studies have shown that the diversity of ENSO spatial patterns (e.g. ‘Central Pacific’ and ‘Eastern Pacific’ El Niño) and intensity (e.g. moderate and extreme El Niño) cause highly different atmospheric responses (e.g. Ciasto *et al* 2015, Yu and Kao 2007, Johnson and Kosaka 2016), the ideal symmetric SST anomalies (figure S5) similar to those used in Trascasa-Castro *et al* (2019) are further used for El Niño (hereafter EN) and La Niña (hereafter LA) simulations. Similar asymmetric features of the PNA-like pattern are still detected (figures 1(g)–(i)), suggesting that the asymmetric circulation responses are robust and mainly arise from the opposite ENSO phases themselves rather than the discrepancy of spatial pattern and magnitude of ENSO forcing.

## 4. Mechanisms of the asymmetry

### 4.1. The asymmetric response of the STJ to El Niño and La Niña

Previous studies have mainly emphasized that the asymmetric impacts of El Niño and La Niña are attributable to the tropical convective heating (e.g. Hoerling *et al* 1997). The convective rainfall anomalies along the equator are located east of the dateline during El Niño, but west during La Niña, due to the active convection threshold (Gadgil *et al* 1984, Johnson and Kosaka 2016). Besides, some studies have stated that the STJ plays an important role in forming the ENSO-induced teleconnection pattern (Simmons *et al* 1983). Therefore, the following questions can be raised that how the STJ varies in different ENSO phases, and how the discrepancy of STJ responses modulates asymmetric atmospheric responses.

Figures 2(a) and (b) display composite zonal mean zonal wind anomalies in boreal winter during El Niño and La Niña years in NCEP2 reanalysis. The climatological STJ is located around 30°N. During El Niño, the zonal mean zonal winds in 200 hPa intensify (weaken) near the equatorial (poleward) flank of the STJ, leading to a strengthening and equatorward contract of the jet. While during La Niña, the jet is weakened and moves poleward due to the weakening (strengthening) of the zonal mean zonal wind near the equatorial (poleward) flank of the STJ. The responses of upper-level zonal winds to ENSO are consistent with the anomalous Hadley cell (HC). In a warm (cold) phase of ENSO,

the HC is strengthening (weakening) and contracted (expanded) owing to the anomalous positive (negative) convective heating in the tropics (figure S6). Figures 2(c) and (d) show the horizontal distribution of upper-level composite zonal winds. The STJ intensifies (weakens) in EN (LA), which corresponds to the changes of zonal mean zonal winds, and the jet core moves eastward (westward) compared to the climatology. The shift of the STJ has been noticed by previous studies (e.g. Rasmusson and Wallace 1983, Yang and Webster 1990, Mo *et al* 1998). According to Yang and Webster (1990) and Rind *et al* (2001), the meridional temperature gradient (figures 2(e) and (f)) largely contributes to the zonal movement of the STJ. Anomalous tropical precipitation in the central and eastern Pacific (figures 2(c) and (d)) causes an increase in the meridional temperature gradient in central subtropical Pacific around 30°N, leading to STJ strengthening and eastward movement of the jet exit in the subtropics during El Niño. While for La Niña, the negative precipitation anomalies induce a decrease in the meridional temperature gradient. Thus the zonal winds in the subtropical Pacific simultaneously decrease. The result is consistent with Rind *et al* (2001) which concluded that the STJ is mainly determined by meridional temperature gradient in the subtropical Pacific but not by the sign of SST anomalies in the tropics.

### 4.2. The impacts of the asymmetric STJ on the zonal shift of ENSO teleconnection

Simmons *et al* (1983) pioneered the idea that barotropic energy conversion between basic mean flow and perturbations at the exit of the STJ plays an important role in the formation of the PNA pattern. In this section, the contribution of the STJ to the asymmetric responses of PNA to El Niño and La Niña is further investigated from the perspective of barotropic energy conversion.

Two LBM experiments are conducted to investigate this issue. Both experiments share the same heat source in the central equatorial Pacific, but different basic states. The horizontal distribution and the vertical profile of the prescribed heat source are presented in figure 3. The only difference between the two is the basic mean flow. As a linearized model, all climatological dynamical and thermodynamical variables are prescribed in the model, e.g. winds, temperature. Climatological winter (DJF) basic states from the NCEP-national center for atmospheric research reanalysis for the period 1980–2005 are utilized in the first experiment (hereafter EXP1), while the basic flow shifts 20-longitude degrees westward in the second experiment (hereafter EXP2). The basic flow in the LBM keeps constant, making it easier to study how the atmospheric circulation responds to tropical heating under different background states.

Figure 4 presents the atmospheric responses in 200 hPa to tropical heating sources under different

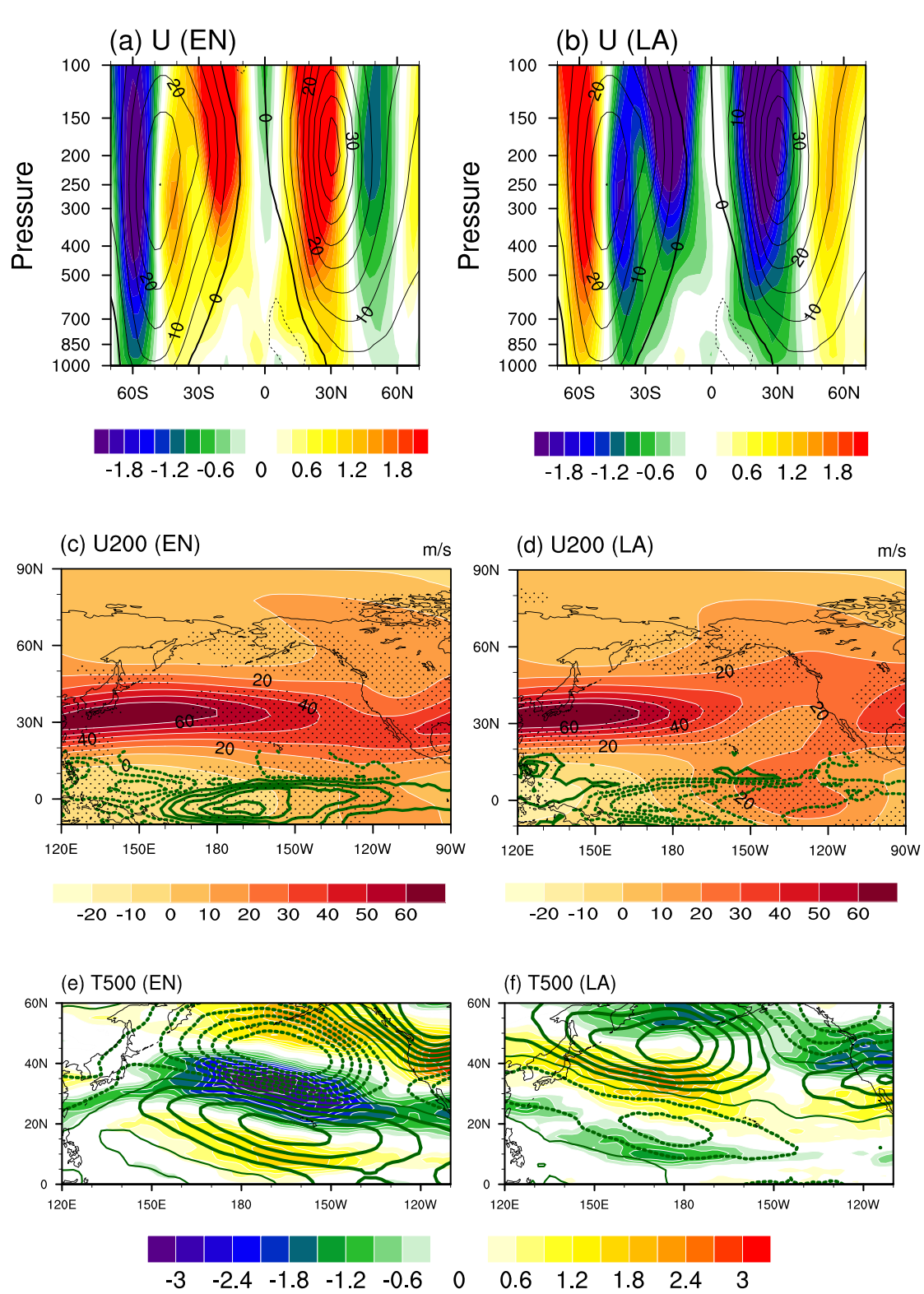


**Figure 2.** Composite DJF zonal mean zonal wind anomalies in (a) EN and (b) LA, contour lines denote the climatology. Composite DJF zonal winds in 200 hPa during (c) El Niño and (d) La Niña, green contour lines denote the precipitation. The meridional temperature gradient (shading;  $^{\circ}\text{C}$ ) and the temperature anomalies in 500 hPa in (e) El Niño and (f) La Niña. The dots denote that the confidence level reaches 95%.

basic mean flow. Upper-level anticyclonic anomalies in tropics and the wave-like disturbances from the subtropical Pacific to North America are well reproduced in EXP1, in high agreement with the observed PNA teleconnection pattern ( $\text{PCC} = 0.83$ ). In EXP1, the atmospheric anomaly in the subtropical north

Pacific mainly concentrated at  $150^{\circ}\text{W}$  and the downstream anticyclone at  $120^{\circ}\text{W}$  in North America (figure 4(a)). While in EXP2, the subtropical and the downstream anomalies move 20-longitude degrees westward (figure 4(b)), accompanied by the movement of the prescribed basic flow. Note

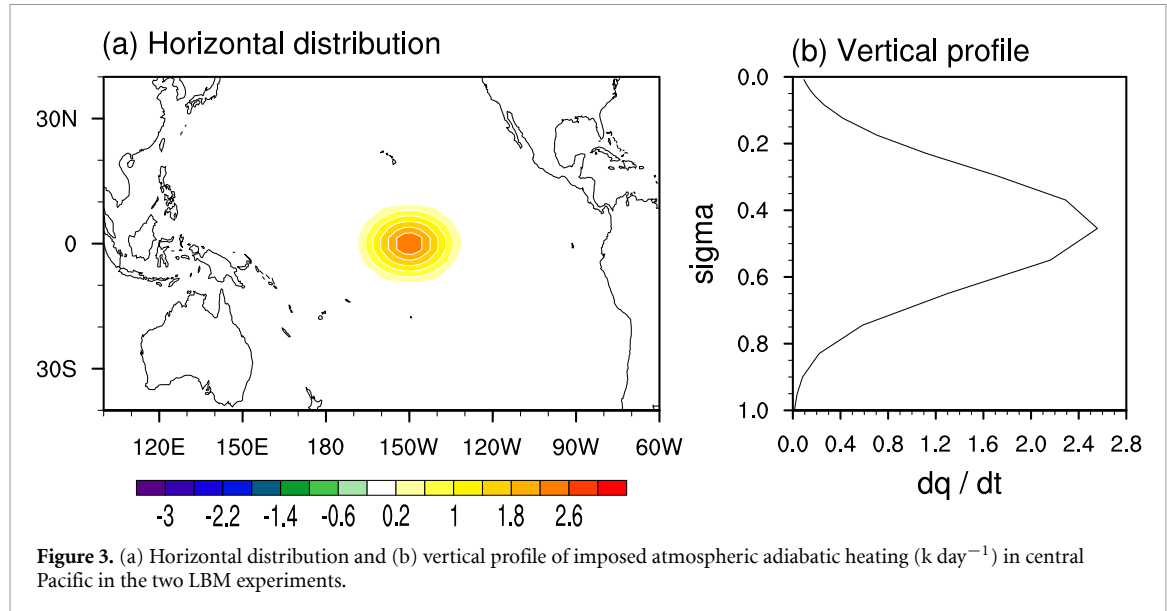


**Figure 3.** (a) Horizontal distribution and (b) vertical profile of imposed atmospheric adiabatic heating ( $\text{k day}^{-1}$ ) in central Pacific in the two LBM experiments.

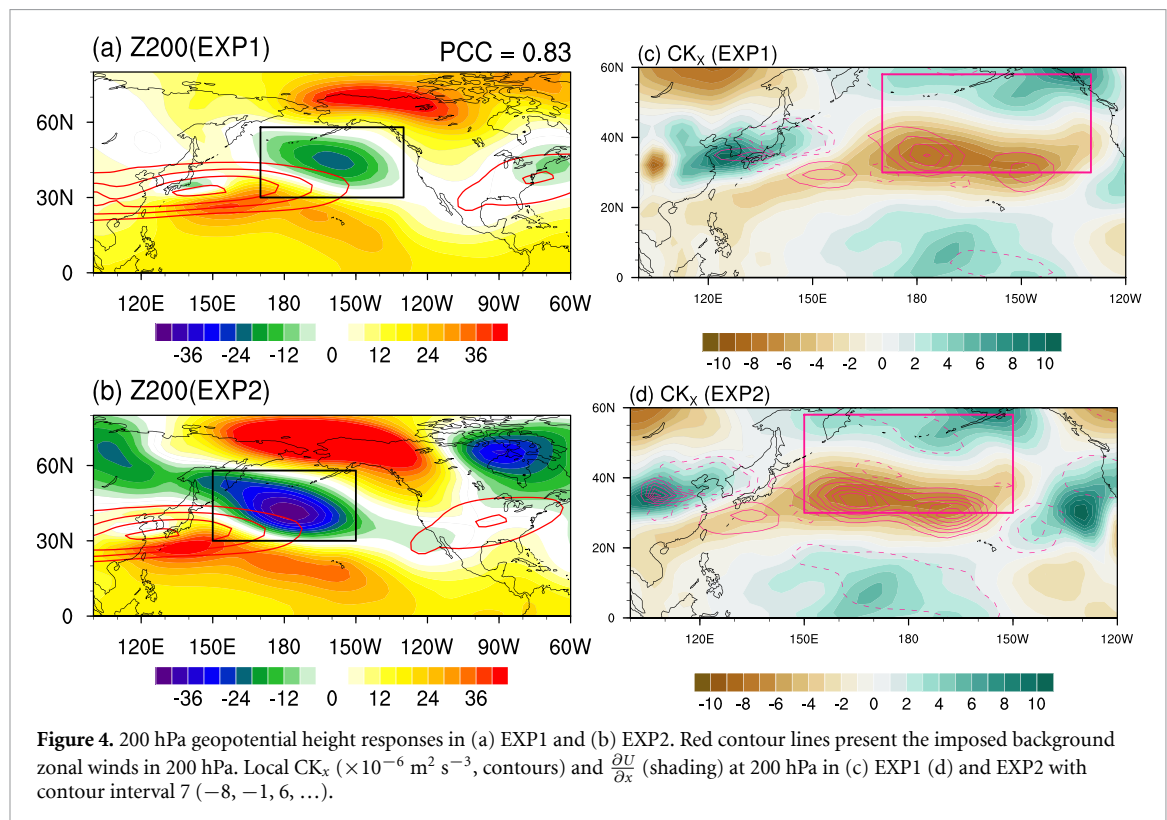


**Figure 4.** 200 hPa geopotential height responses in (a) EXP1 and (b) EXP2. Red contour lines present the imposed background zonal winds in 200 hPa. Local  $CK_x$  ( $\times 10^{-6} \text{ m}^2 \text{ s}^{-3}$ , contours) and  $\frac{\partial U}{\partial x}$  (shading) at 200 hPa in (c) EXP1 (d) and EXP2 with contour interval 7 ( $-8, -1, 6, \dots$ ).

that the downstream anticyclone located in western America in EXP2 is more northward relative to that in EXP1. The discrepancy mainly originates from the idealized change of the basic state in EXP2. The movement of the basic state may influence the wave propagation in the downstream region. However, as we are primarily concerned with the overall movement of the wave trains in this study, the discrepancy would not have a significant impact on the findings and conclusions. To further investigate how the asymmetric STJ contributes to the movement of the PNA patterns, barotropic energy conversion is introduced.

As Kosaka and Nakamura (2006), the barotropic growth of the local kinetic energy (KE) associated with perturbations from the basic state is given by:

$$\begin{aligned} \frac{\partial \text{KEH}}{\partial t} &\approx \underbrace{\frac{(v'^2 - u'^2)}{2} \left( \frac{\partial u_b}{\partial x} - \frac{\partial v_b}{\partial y} \right)}_{CK_x} \\ &\quad - u'v' \underbrace{\left( \frac{\partial u_b}{\partial y} + \frac{\partial v_b}{\partial x} \right)}_{CK_y} \end{aligned} \quad (1)$$

here  $u'$  and  $v'$  are the anomalous zonal and meridional winds.  $u_b$  and  $v_b$  denote the climatological winds. KEH is horizontal perturbed kinetic energy, and CK (the sum of  $CK_x$  and  $CK_y$ ) is the conversion of local kinetic energy from the basic state to perturbations. Based on equation (1), the dominant pathways by which the atmospheric anomalies extract kinetic energy from the basic state can be described in term of two terms:  $CK_x$  and  $CK_y$ . At the exit of the jet, where the zonal wind converges into a broad region,  $\frac{\partial u_b}{\partial x}$  is strong negative. Thus, zonally elongated circulation anomalies ( $u'^2 > v'^2$ ) can readily extract positive  $CK_x$  in the STJ exit region according to equation (1).

As  $CK_x$  is dominant in the subtropics especially at the exit region of the STJ, only  $CK_x$  is presented in this study. The spatial pattern and magnitude of CK highly resembles  $CK_x$ . Figures 4(c) and (d) display the  $CK_x$  and  $\frac{\partial u_b}{\partial x}$  in EXP1 and EXP2, respectively. Pronounced positive  $CK_x$  distributes between  $170^{\circ}\text{E} \sim 140^{\circ}\text{W}$ , at the exit of the STJ in both experiments, where  $\frac{\partial u_b}{\partial x}$  is strong negative. In this region, the zonal elongated disturbance can extract barotropic energy ( $CK_x$ ) from the basic flow and thus efficiently develops (figure 4). Compared with EXP1, in EXP2 where the basic flow is shift 20-longitude degrees westward, the zonal wind convergent region and the associated strong positive  $CK_x$  correspondingly move about 20-longitude degrees westward. As a result, the region where disturbance easily extracts kinetic energy also shifts to the west, leading to the westward movement of the PNA-like pattern. The consistency of strong positive  $CK_x$  and atmospheric anomaly suggests that the strong barotropic energy conversion contributes to the development of disturbance in the STJ exit region, and could anchor the location of the related wave trains.

The above results demonstrate that, besides the convection location, the STJ exit could anchor the location of the extratropical teleconnection. One might ask, which has more influence on the movement of the wave train, the tropical convective position or the STJ? Another experiment (hereafter EXP3) forced by the same climatological basic state as EXP1, but different heating source centering in  $170^{\circ}\text{W}$  is performed to investigate the issue. As shown in figure S7, the tropical Gill-like response shifts westward in EXP3 relative to EXP1. However, the extratropical perturbation has little change and still anchors at the exit of the STJ. The result is somewhat unexpected but is consistent with the landmark work of Simmons *et al* (1983) and Ting and Yu (1998). Another experiment with negative heating is also conducted, and similar results are obtained (figure S7(c)). Note that LBM is only a linear dry model without moist process and nonlinear feedback, so the above results should be cautiously explained.

## 5. Conclusions and discussion

This study investigates the asymmetry of ENSO-related waves in the Northern Hemisphere in boreal winter and the involved physical and dynamical basis from the perspective of energy conversion. In boreal winter, the extratropical atmospheric responses during El Niño years are more eastward compared to La Niña, which leads to significant differences in the regions influenced by ENSO in the United States. The asymmetric features are highly reproduced by atmospheric general circulation model (AGCM) experiments forced with composite SST and idealized symmetric SST, indicating the asymmetric impact is robust and mainly arises from difference ENSO phases rather than different spatial patterns and intensity of the forcing.

Different from previous studies that focus on tropical convective heating, the study presents that the asymmetric STJ in El Niño and La Niña contributes to the zonal movement of the ENSO-triggered teleconnection pattern. From the perspective of energy conversion, the atmospheric anomalies readily extract kinetic energy and develop efficiently at the exit of the STJ. As the central-eastern tropical Pacific warms up (cools down) and the meridional temperature gradient increases (decreases), the STJ shifts eastward (westward) accordingly. The movement of the STJ leads to the shift of the location where disturbance develops most efficiently, ultimately contributing to the asymmetry of the teleconnection pattern.

LBM experiments suggest that the role of varying STJ may be greater than the movement of the location of the heat source. However, as LBM is only a linear dry model without moist process and nonlinear feedback, the results should be cautiously explained. More experiments by linear models and comprehensive models should be conducted to further investigate the issue.

In addition, some other variabilities (e.g. ‘Arctic Oscillation’, ‘Atlantic Multi-decadal Oscillation’) may also modulate PNA-like wave trains (e.g. Zhang and Delworth 2007, Pinto *et al* 2011). The effects of other variabilities on the PNA wave train should be further investigated in the future.

## Data availability statement

The data that supports the finding of this study is openly available at <https://psl.noaa.gov/data/gridded/data.ncep.reanalysis2.html> (NCEP2; Kanamitsu *et al* 2002).

The data that support the findings of this study are available upon reasonable request from the authors.

## Acknowledgments

The author would like to thank the two anonymous reviewers for many useful comments. Wang Ya would like to thank Professor Ding Qinghua for many useful discussions. The study is jointly supported by National Natural Science Foundation of China (41831175), the National Key R&D Program of China (2018YFA0605904 and 2019YFA0606703), the Strategic Priority Research Program of Chinese Academy of Sciences (XDA20060502), the National Natural Science Foundation of China (41775086), Key Deployment Project of Centre for Ocean MegaResearch of Science, Chinese Academy of Sciences (COMS2019Q03), and Youth Innovation Promotion Association of CAS. The authors declare no competing interest.

## ORCID iDs

- Ya Wang  <https://orcid.org/0000-0003-1527-5413>  
 Kaiming Hu  <https://orcid.org/0000-0002-9988-5747>  
 Gang Huang  <https://orcid.org/0000-0002-8692-7856>

## References

- Adames Á F and Wallace J M 2017 On the tropical atmospheric signature of El Niño *J. Atmos. Sci.* **74** 1923–39  
 Ciausto L M, Simpkins G R and England M H 2015 Teleconnections between Tropical Pacific SST Anomalies and Extratropical Southern Hemisphere Climate *Journal of Climate* **28** 56–65  
 Dong B, Dai A, Vuille M and Timm O E 2018 Asymmetric modulation of ENSO teleconnections by the interdecadal Pacific oscillation *J. Clim.* **31** 7337–61  
 Gadgil S, Joseph P V and Joshi N V 1984 Ocean–atmosphere coupling over monsoon regions *Nature* **312** 141–3  
 Held I M, Ting M F and Wang H L 2002 Northern winter stationary waves: theory and modeling *J. Clim.* **15** 2125–44  
 Henley B J, Gergis J, Karoly D J, Power S B, Kennedy J and Folland C K 2015 A tripole index for the interdecadal Pacific oscillation *Clim. Dyn.* **45** 3077–90  
 Hoerling M P, Kumar A and Zhong M 1997 El Niño, La Niña, and the nonlinearity of their teleconnections *J. Clim.* **10** 1769–86  
 Horel J D and Wallace J M 1981 Planetary-scale atmospheric phenomena associated with the Southern Oscillation *Monthly Weather Rev.* **109** 813–29  
 Hoskins B J, McIntyre M E and Robertson A W 1985 On the use and significance of isentropic potential vorticity maps *Q. J. R. Meteorol. Soc.* **111** 877–946  
 Hu K, Huang G, Huang P, Kosaka Y and Xie S-P 2021 Intensification of El Niño-induced atmospheric anomalies under greenhouse warming *Nat. Geosci.* **14** 377–82  
 Hu K, Huang G, Xie S-P and Long S-M 2019 Effect of the mean flow on the anomalous anticyclone over the Indo-Northwest Pacific in post-El Niño summers *Clim. Dyn.* **53** 5725–41  
 Huang B *et al* 2017 Extended Reconstructed Sea Surface Temperature, Version 5 (ERSSTv5): Upgrades, Validations, and Intercomparisons *J. Clim.* **30** 8179–205  
 Jia X, Ge J and Wang S 2016 Diverse impacts of ENSO on wintertime rainfall over the maritime continent *Int. J. Climatol.* **36** 3384–97  
 Johnson N C and Kosaka Y 2016 The impact of eastern equatorial Pacific convection on the diversity of boreal winter El Niño teleconnection patterns *Clim. Dyn.* **47** 3737–65  
 Kanamitsu M, Ebisuzaki W, Woollen J, Yang S, Hnilo J J, Fiorino M and Potter G L 2002 NCEP–DOE AMIP-II Reanalysis (R-2) *Bull. Amer. Meteor. Soc.* **83** 1631–44  
 Kosaka Y and Nakamura H 2006 Structure and dynamics of the summertime Pacific–Japan teleconnection pattern *Q. J. R. Meteorol. Soc.* **132** 2009–30  
 Liu Z and Alexander M 2007 Atmospheric bridge, oceanic tunnel, and global climatic teleconnections *Rev. Geophys.* **45**  
 Mo R, Fyfe J and Derome J 1998 Phase-locked and asymmetric correlations of the wintertime atmospheric patterns with the ENSO *Atmosphere-Ocean* **36** 213–39  
 Pinto J G, Reyers M and Ulbrich U 2011 The variable link between PNA and NAO in observations and in multi-century CGCM simulations *Clim. Dyn.* **36** 337–54  
 Rao J and Ren R 2016 Asymmetry and nonlinearity of the influence of ENSO on the northern winter stratosphere: 2. Model study with WACCM *J. Geophys. Res.* **121** 9017–32  
 Rasmusson E M and Wallace J M 1983 Meteorological aspects of the El Niño/Southern Oscillation *Science* **222** 1195–202  
 Rind D, Chandler M, Lerner J, Martinson D G and Yuan X 2001 Climate response to basin-specific changes in latitudinal temperature gradients and implications for sea ice variability *J. Geophys. Res.* **106** 20161–73  
 Roeckner E *et al* 2003 *The atmospheric general circulation model ECHAM 5. Part I: model description* Rep. 349, p 140 Max-Planck-Institut für Meteorologie  
 Seager R, Harnik N, Kushnir Y, Robinson W and Miller J 2003 Mechanisms of hemispherically symmetric climate variability *J. Clim.* **16** 2960–78  
 Simmons A J, Wallace J M and Branstator G W 1983 Barotropic wave-propagation and instability, and atmospheric teleconnection patterns *J. Atmos. Sci.* **40** 1363–92  
 Tao W, Huang G, Wu R, Hu K, Wang P and Chen D 2016 Asymmetry in summertime atmospheric circulation anomalies over the northwest Pacific during decaying phase of El Niño and La Niña *Clim. Dyn.* **49** 2007–23  
 Ting M F and Yu L H 1998 Steady response to tropical heating in wavy linear and nonlinear baroclinic models *J. Atmos. Sci.* **55** 3565–82  
 Trascasa-Castro P, Maycock A C, Yiu Y Y S and Fletcher J K 2019 On the linearity of the stratospheric and Euro-Atlantic sector response to ENSO *J. Clim.* **32** 6607–26  
 Trenberth K E, Branstator G W, Karoly D, Kumar A, Lau N C and Ropelewski C 1998 Progress during TOGA in understanding and modeling global teleconnections associated with tropical sea surface temperatures *J. Geophys. Res.* **103** 14291–324  
 Watanabe M and Kimoto M 2000 Atmosphere-ocean thermal coupling in the North Atlantic: a positive feedback *Q.J.R. Meteorol. Soc.* **126** 3343–69  
 Xie S-P, Kosaka Y, Du Y, Hu K, Chowdary J S and Huang G 2016 Indo-western Pacific ocean capacitor and coherent climate anomalies in post-ENSO summer: a review *Adv. Atmos. Sci.* **33** 411–32  
 Yang S and Webster P J 1990 The effect of summer tropical heating on the location and intensity of the extratropical westerly jet streams *J. Geophys. Res.* **95** 18705–21  
 Yang X and Huang P 2021 Restored relationship between ENSO and Indian summer monsoon rainfall around 1999/2000 *The Innovation* **2** 100102  
 Yu J-Y and Kao H-Y 2007 Decadal changes of ENSO persistence barrier in SST and ocean heat content indices: 1958–2001 *J. Geophys. Res.* **112** D13106  
 Zhang R and Delworth T L 2007 Impact of the Atlantic multidecadal oscillation on North Pacific climate variability *Geophys. Res. Lett.* **34** L23708